

the same general behavior as experimentally observed for $\text{Gd}(\text{hfac})_3\text{NITR}$.

The results of the calculations for $J_{\text{Gd-R}} > 0$ are similar to that described above, with a diverging behavior in the ferrimagnetic regime ($J_{\text{R-R}} = 0$ and $J_{\text{Gd-Gd}} = 0$), a frustrated behavior when $J_{\text{R-R}} > 0$ and $J_{\text{Gd-Gd}} = 0$, and a monotonically decreasing behavior when a weak antiferromagnetic coupling between gadolinium ions is turned on.

Starting from the encouraging conclusions of the sample calculations, we attempted a quantitative fit of the magnetic data for $\text{Gd}(\text{hfac})_3\text{NITeT}$ and $\text{Gd}(\text{hfac})_3\text{NITiPr}$ that yielded $J_{\text{Gd-R}} = -0.41 \text{ cm}^{-1}$, $J_{\text{R-R}} = 5.08 \text{ cm}^{-1}$, and $J_{\text{Gd-Gd}} = 0.98 \text{ cm}^{-1}$ for the former and $J_{\text{Gd-R}} = -0.42 \text{ cm}^{-1}$, $J_{\text{R-R}} = 5.32 \text{ cm}^{-1}$, and $J_{\text{Gd-Gd}} = 0.38 \text{ cm}^{-1}$ for the latter. In the limit imposed by the intrinsic inadequacy of the Ising model for interpreting the data of a system made up by highly isotropic species, these results can be considered satisfactory. In fact the $J_{\text{Gd-R}}$ and $J_{\text{R-R}}$ values compare well with those previously reported for other mononuclear gadolinium-radical complexes.³⁴ The $J_{\text{Gd-Gd}}$ constants are fairly large for interactions between rare-earth ions, but comparable values have been recently observed from inelastic neutron-scattering measurements in rare-earth pairs.³⁸ The fact that a nnn coupling constant, namely $J_{\text{Gd-Gd}}$ in $\text{Gd}(\text{hfac})_3\text{NITeT}$, is larger than the nn coupling constant could be at first sight surprising; it must however be taken into account that the comparison should be made between the constants scaled by a factor $1/n_1n_2$, where n_1 and n_2 are the number of electron on the first and on the second interacting centers, respectively; moreover, we are in this case comparing coupling constants that derive from different exchange mechanisms. Further, it must be recalled that the two NO groups of the radical are equivalent; therefore, a superexchange interaction

is effectively transmitted to the two ends of the nitronyl nitroxide. The difference between the $J_{\text{Gd-Gd}}$ constants obtained in the two cases can be tentatively attributed to the different intrachain Gd-Gd distances in the two derivatives. Actually for $\text{Gd}(\text{hfac})_3\text{NITeT}$ two different Gd-Gd distances are observed namely 8.59 and 8.64 Å, while in $\text{Gd}(\text{hfac})_3\text{NITiPr}$ the Gd-Gd intrachain distance is 8.88 Å.

Conclusions

The $\text{Gd}(\text{hfac})_3\text{NITR}$ (R = ethyl, isopropyl) compounds represent unique one-dimensional magnetic materials in which nnn interactions determine the preferred spin orientation at low temperature. Within the simple Ising model that we worked out quantitatively, the ground state corresponds to a two-spins-up, two-spins-down configuration, but it cannot be excluded that within a more correct Heisenberg exchange approach the ground state is characterized by a more complicated spin arrangement.¹⁰ Presumably, neutron diffraction studies could provide a definitive answer to this problem. The rapid increase of the EPR line width below 20 K may be in fact indicative of peculiar spin dynamics associated with the ground state.

It is very important to notice how the magnetic interactions between rare-earth ions and organic radicals give rise to unexpected behaviors, which are due to the fact that the interactions between metal ions and radicals are relatively weak, while the superexchange between radicals through the metal ions (and between metal ions through the radicals) is relatively strong.

Acknowledgment. Thanks are expressed to MURST, to the CNR, and to the Progetto Finalizzato "Materiali Speciali per Tecnologie Avanzate" for financing the research.

Supplementary Material Available: Listings of crystallographic and experimental data (Table SI), complete bond distances and angles (Table SII), and anisotropic thermal parameters (Table SIII) (6 pages); a table of observed and calculated structure factors (Table SIV) (13 pages). Ordering information is given on any current masthead page.

(38) Doenni, A.; Furrer, A.; Blank, H.; Heidemann, A.; Gudel, H. U. *J. Phys.* **1988**, *49*, C8-1513.

Contribution from the Department of Chemistry, University of Florence, Florence, Italy, and Departement de Recherche Fondamentale, Centre d'Etudes Nucleaires, Grenoble, France

Structure and Magnetic Properties of Manganese(II) Carboxylate Chains with Nitronyl Nitroxides and Their Reduced Amidino-Oxide Derivatives. From Random-Exchange One-Dimensional to Two-Dimensional Magnetic Materials

Andrea Caneschi,^{1a} Dante Gatteschi,^{*1a} Maria Chiara Melandri,^{1a} Paul Rey,^{1b} and Roberta Sessoli^{1a}

Received February 20, 1990

Two compounds of formula $\text{Mn}(\text{pfpr})_2(\text{NITMe})$ (I) and $[\text{Mn}(\text{pfpr})_2]_2(\text{NITMe})(\text{IMHMe})$ (II), respectively, where pfpr = pentafluoropropionate, NITMe = 2,4,4,5,5-pentamethyl-4,5-dihydro-1H-imidazolyl-1-oxyl 3-oxide, and IMHMe = 2,4,4,5,5-pentamethyl-4,5-dihydroimidazole 3-oxide, have been synthesized. The latter crystallizes in the monoclinic $P2_1/c$ space group with $a = 13.898$ (3) Å, $b = 19.089$ (4) Å, $c = 7.867$ (3) Å, $\beta = 94.90$ (2)°, $R = 0.052$, and $Z = 4$. The structure consists of manganese carboxylate chains that have as additional bridging ligands NITMe and IMHMe molecules randomly distributed along the chains. Hydrogen bonds between neighboring pairs of NITMe and IMHMe molecules connect the chains in puckered planes perpendicular to a . The magnetic properties of $[\text{Mn}(\text{pfpr})_2]_2(\text{NITMe})(\text{IMHMe})$ are consistent with a random-exchange one-dimensional model, while those of $\text{Mn}(\text{pfpr})_2(\text{NITMe})$ indicate a two-dimensional system with antiferromagnetic interactions between ferrimagnetic chains. The magnetic properties suggest that the crystal structure of I is similar to that of II with the hydrogen bonds replaced by longer contacts between noncoordinated NO groups of the radicals.

Introduction

The so-called metal-radical approach has been successfully employed in the synthesis of molecular based ferromagnets.² It consists in the use of stable organic radicals such as the nitronyl nitroxides, 2-R-4,4,5,5-tetramethyl-4,5-dihydro-1H-imidazolyl-1-oxyl 3-oxide, NITR, as ligands for transition-metal ions, which

can thus be connected in infinite structures. The individual metal-radical coupling can be either ferro- or antiferromagnetic, and in this way one-dimensional ferro- and ferrimagnets were obtained.²⁻⁵ In a few cases these were found to undergo a phase

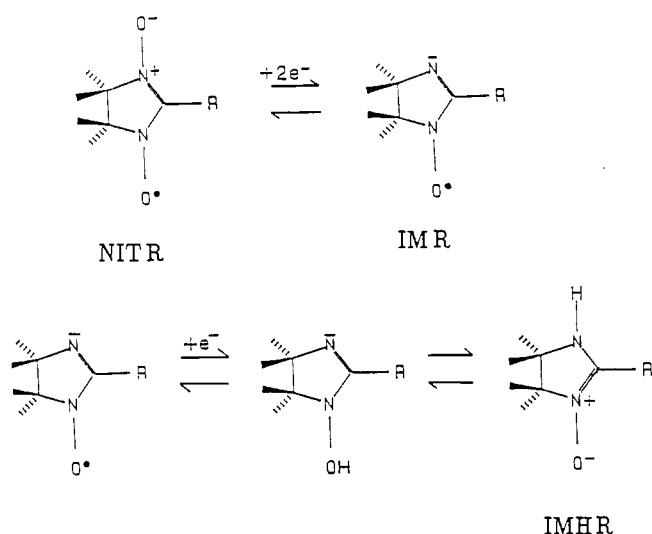
(1) (a) University of Florence. (b) Centre d'Etudes Nucleaires.
(2) Caneschi, A.; Gatteschi, D.; Sessoli, R.; Rey, P. *Acc. Chem. Res.* **1989**, *22*, 392.

(3) Caneschi, A.; Gatteschi, D.; Laugier, J.; Rey, P. *J. Am. Chem. Soc.* **1987**, *109*, 2191.

(4) Caneschi, A.; Gatteschi, D.; Rey, P.; Sessoli, R. *Inorg. Chem.* **1988**, *27*, 1756.

(5) Caneschi, A.; Gatteschi, D.; Renard, J.-P.; Rey, P.; Sessoli, R. *Inorg. Chem.* **1989**, *28*, 2940.

Scheme I



transition to three-dimensional ferromagnetic order in the range 4–8 K.^{5–7}

In principle there are no difficulties for the design of materials that undergo magnetic phase transitions at higher temperatures: the network of coupled metal ions and radicals should be extended from one to two and three dimensions,⁸ and the strong magnetic coupling between the paramagnetic centers would ensure high transition temperatures. However, the synthetic problem is by no means trivial and it features one of the challenges to modern chemical ingenuity, that of learning how to control the synthesis of extended systems in a desired fashion in order to extend the properties from the individual building blocks to the whole lattice.

The main limitations we have found so far in our use of nitronyl nitroxides, in order to synthesize bulk ferro- or ferrimagnets, are related to their weak Lewis basicity, which requires relatively strong Lewis acids in order to form stable compounds. So we found it was relatively easy to react the nitroxides with metal hexafluoroacetylacetonates, $\text{M}(\text{hfac})_2$, but with this approach only one-dimensional magnetic materials can be obtained. The metal nitroxide chains are well shielded from each other by the bulky CF_3 groups, and the transition temperatures to three-dimensional magnetic order are relatively low.

In order to increase the critical temperatures of the systems we decided to use metal carboxylates instead of metal hexafluoroacetylacetonates, because the carboxylates have a large tendency to bridge metal ions, thus in principle forming two- and three-dimensional structures. Using this approach, we synthesized compounds of formula $[\text{Mn}(\text{pfbz})_2]_2(\text{NITR})$, where pfbz = pentafluorobenzoate and $\text{R} = \text{Me}$ and Et , which order magnetically at ca. 25 K.⁹ Unfortunately, no crystal suitable for X-ray analysis could be obtained, so that the considerations on the nature of the exchange interactions remained speculative.

With $\text{Mn}(\text{pfpr})_2$ (pfpr = pentafluoropropionate), we obtained a dinuclear complex of formula $\text{Mn}(\text{pfpr})_2(\text{NITe})_2(\text{H}_2\text{O})_3$,¹⁰ in which the two metal ions are bridged by two carboxylates and one additional ligand, which is well-known in other polynuclear carboxylates^{11–14} and also in biological systems such as the active

Table I. Crystal Data and Experimental Parameters for $[\text{Mn}(\text{pfpr})_2]_2(\text{NITMe})(\text{IMHMe})$

formula	$\text{Mn}_2\text{C}_{28}\text{H}_{31}\text{N}_4\text{O}_{11}\text{F}_{20}$	space group	$P2_1/c$
fw	1089.41	T	25°C
a	$13.898(3)\text{ \AA}$	λ	0.71073 \AA ($\text{Mo K}\alpha$)
b	$19.089(4)\text{ \AA}$	ρ_{calcd}	1.740 g/cm^3
c	$7.867(3)\text{ \AA}$	μ	5.80 cm^{-1}
β	$94.90(2)^\circ$	$R(F_o)$	0.052
V	2079 \AA^3	$R_w(F_o)$	0.058
Z	2		

site of hemerythrin.¹⁵ In $\text{Mn}(\text{pfpr})_2(\text{NITe})_2(\text{H}_2\text{O})_3$ the ligand L is a water molecule, and this has been the first example of a dinuclear μ -aquo d^5 complex. The analysis¹⁰ of the magnetic properties of this compound and the comparison with the data reported for other dinuclear complexes showed that in bis(μ -carboxylato) complexes the antiferromagnetic exchange coupling decreases by approximately 1 order of magnitude at each step in the series $\text{O}^{2-} > \text{OH}^- > \text{H}_2\text{O}$.

We have now isolated two compounds of formula $\text{Mn}(\text{pfpr})_2(\text{NITMe})$ (I) and $[\text{Mn}(\text{pfpr})_2]_2(\text{NITMe})(\text{IMHMe})$ (II), where IMHMe ($\text{IMHMe} = 2,4,4,5,5$ -pentamethyl-4,5-dihydroimidazole 3-oxide) is the reduced form of the radical of formula shown in Scheme I, which reports also the redox pathway connecting NITMe to IMHMe , through the intermediate IMMe radical.^{16–18} The final reduced species IMHMe can in principle exist in two tautomeric forms, i.e. amidino-oxide and imino-hydroxylamine, of which the former seems the most stable.^{16,17} The two compounds have structures with magnetic dimensionality that is larger than one, as shown by the X-ray crystal structure of the latter, which is the only one for which we were able to grow suitable single crystals. The interest of the structure of $[\text{Mn}(\text{pfpr})_2]_2(\text{NITMe})(\text{IMHMe})$ is that it contains both the radical and its reduced form, which are bound to the same metal ion in a very similar fashion, in such a way that the differences show up only as disorder in the structure. As we will show in this compound, metal carboxylate chains are connected in a two-dimensional lattice by hydrogen bonds, showing how complex supramolecular structures¹⁹ can spontaneously be assembled in the solid state.

Experimental Section

Synthesis of the Complexes. $\text{Mn}(\text{pfpr})_2 \cdot 2\text{H}_2\text{O}$ was prepared by mixing a water solution of $\text{Mn}(\text{CO}_3) \cdot n\text{H}_2\text{O}$ with the stoichiometric amount of pentafluoropropionic acid; the solution was filtered and boiled to obtain an oil, which was dried under vacuum. The NITMe radical was prepared according to the literature.^{16,20}

Compound I was prepared by dissolving 1 mmol of $\text{Mn}(\text{pfpr})_2 \cdot 2\text{H}_2\text{O}$ in 120 mL of boiling CHCl_3 ; the solution was allowed to cool down for some minutes before adding 1 mmol of NITMe . Immediately an orange-red precipitate appeared, which was filtered out and washed with heptane. The yield was about 80%. The compound analyzed satisfactorily for $\text{Mn}(\text{pfpr})_2(\text{NITMe})$. Anal. Calcd for $\text{C}_{14}\text{H}_{15}\text{N}_2\text{O}_6\text{F}_{10}\text{Mn}$: C, 30.45; H, 2.74; N, 5.07. Found: C, 30.26; H, 2.45; N, 4.89.

Compound II was prepared by dissolving 1 mmol of $\text{Mn}(\text{pfpr})_2 \cdot 2\text{H}_2\text{O}$ in 250 mL of boiling CHCl_3 ; 1 mmol of NITMe was added under stirring after 1 min, and the solution was allowed to cool down to room temperature very slowly. Nice ruby red crystals were obtained after 2 weeks, and the yield was evaluated at about 50%. The compound analyzed satisfactorily for $[\text{Mn}(\text{pfpr})_2]_2(\text{NITMe})(\text{IMHMe})$. Anal. Calcd for $\text{C}_{28}\text{H}_{31}\text{N}_4\text{O}_{11}\text{F}_{20}\text{Mn}_2$: C, 30.87; H, 2.87; N, 5.14. Found: C, 30.56; H, 2.68; N, 4.98.

Optical Spectra. Electronic spectra were recorded in the range 15000–25000 cm^{-1} on a Perkin-Elmer Lambda 9 spectrophotometer.

- Caneschi, A.; Gatteschi, D.; Renard, J.-P.; Rey, P.; Sessoli, R. *Inorg. Chem.* **1989**, *28*, 1976.
- Caneschi, A.; Gatteschi, D.; Renard, J.-P.; Rey, P.; Sessoli, R. *Inorg. Chem.* **1989**, *28*, 3314.
- Stanley, H. E. *Introduction to Phase Transitions and Critical Phenomena*; Clarendon Press: Oxford, England, 1971.
- Caneschi, A.; Gatteschi, D.; Renard, J.-P.; Rey, P.; Sessoli, R. *J. Am. Chem. Soc.* **1989**, *111*, 785.
- Caneschi, A.; Ferraro, F.; Gatteschi, D.; Melandri, M. C.; Rey, P.; Sessoli, R. *Angew. Chem., Int. Ed. Engl.* **1989**, *28*, 1365.
- Wiegardt, K.; Bossek, U.; Bonvoisin, J.; Beauvillain, P.; Girerd, J. J.; Nuber, B.; Weiss, J.; Heize, J. *Angew. Chem., Int. Ed. Engl.* **1983**, *25*, 1030.
- Armstrong, W. K.; Lippard, S. J. *J. Am. Chem. Soc.* **1984**, *106*, 4632.

- Hartman, J. A. R.; Rardin, R. L.; Chaudhuri, P.; Pohl, K.; Wiegardt, K.; Nuber, B.; Weiss, J.; Papaefthymiou, G. C.; Frankel, R. B.; Lippard, S. J. *J. Am. Chem. Soc.* **1987**, *109*, 7387.
- Wiegardt, K.; Pohl, K.; Ventur, D. *Angew. Chem., Int. Ed. Engl.* **1985**, *24*, 392.
- Klotz, I. M.; Kurtz, D. M., Jr. *Acc. Chem. Res.* **1984**, *17*, 17.
- Ullman, E. F.; Call, L.; Osiecky, J. K. *J. Org. Chem.* **1970**, *35*, 3623.
- Ullman, E. F.; Osiecky, J. K.; Boocock, D. J. B.; Darcy, R. J. *Am. Chem. Soc.* **1972**, *74*, 7049.
- Caneschi, A.; Gatteschi, D.; Laugier, J.; Rey, P.; Zanchini, C. *Inorg. Chem.* **1989**, *28*, 1969.
- Lehn, J.-M. *Angew. Chem., Int. Ed. Engl.* **1988**, *27*, 89.
- Lamchen, M.; Wittag, T. W. *J. Chem. Soc.* **1966**, 2300.

Table II. Atomic Positional Parameters ($\times 10^4$) and Isotropic Thermal Factors ($\text{\AA}^2 \times 10^3$) for $[\text{Mn}(\text{pfpr})_2]_2(\text{NITMe})(\text{IMHMe})^a$

	x/a	y/b	z/c	U_{iso}
Mn	2236 (1)	2471 (1)	2545 (1)	36
O1	2313 (3)	1868 (2)	5130 (5)	35
O2	4332 (7)	-43 (5)	5003 (16)	63
O3	1018 (4)	2994 (3)	3370 (6)	52
O4	1178 (4)	3181 (3)	6175 (6)	56
O5	3357 (3)	1817 (3)	1642 (6)	42
O6	3299 (3)	1833 (3)	-1232 (5)	42
N1	2632 (4)	1200 (3)	5124 (7)	36
N2	3595 (4)	310 (3)	5043 (8)	46
C1	3539 (5)	1016 (3)	5163 (8)	36
C2	1975 (5)	572 (4)	5266 (10)	47
C3	2624 (5)	3 (4)	4561 (10)	52
C4	4363 (5)	1491 (1)	5304 (9)	42
C5	1010 (5)	702 (5)	4419 (13)	70
C6	1885 (7)	445 (5)	7196 (11)	72
C7	2470 (7)	0 (6)	2601 (10)	84
C8	2522 (7)	-728 (4)	5226 (14)	77
C9	752 (5)	3207 (4)	4727 (9)	41
C10	-227 (6)	3596 (4)	4619 (11)	58
C11	-1001 (9)	3257 (7)	5531 (16)	92
C12	3612 (5)	1651 (3)	226 (9)	36
C13	4489 (5)	1134 (4)	285 (9)	38
C14	5465 (6)	1490 (4)	382 (12)	59
F1	-588 (4)	3665 (4)	2976 (7)	114
F2	-98 (5)	4255 (3)	5208 (9)	106
F3	-775 (5)	3325 (5)	7210 (9)	132
F4	-1842 (4)	3578 (5)	5217 (11)	159
F5	-1056 (5)	2588 (4)	5170 (12)	146
F6	4501 (3)	716 (2)	1666 (5)	60
F7	4427 (3)	712 (2)	-1091 (5)	59
F8	5607 (4)	1882 (3)	1763 (7)	94
F9	5530 (4)	1917 (3)	-923 (8)	93
F10	6165 (3)	1027 (3)	388 (9)	102

Infrared spectra were recorded on a Perkin-Elmer 283 spectrometer.

X-ray Structure Determination. X-ray data for $[\text{Mn}(\text{pfpr})_2]_2(\text{NITMe})(\text{IMHMe})$ (II) were collected on an Enraf-Nonius CAD-4 four-circle diffractometer with Mo $K\alpha$ radiation. Accurate unit cell parameters were derived from least-squares refinement of the setting angles of 23 reflections ($8^\circ \leq \theta \leq 17^\circ$) and are reported in Table I with other experimental parameters. A more complete listing of experimental parameters is given as supplementary material. Data were corrected for Lorentz and polarization effects but not for absorption and extinction. The systematic absences revealed that the compound belongs to the monoclinic system, space group $P2_1/c$.

The crystal structure was solved by conventional Patterson and Fourier methods with the SHELX-76 package.²¹ A Patterson map enabled us to localize the manganese atom; the positions of the other non-hydrogen atoms were found by successive Fourier and difference Fourier synthesis. Due to the small number of reflections with $F_o \geq 4\sigma(F_o)$ anisotropic thermal parameters were introduced only for the manganese and fluorine atoms, for the carbon atoms of the CF_3 groups and for the nitrogen atoms of the NO groups not bonded to the metal atom.

The asymmetric unit contains one manganese ion, two carboxylates, and a molecule intermediate between NITMe and IMHMe. Attempts were made to refine the structure with the space group Pc and a double asymmetric unit, but the value of R remained greater than 0.08 and the differences between the two molecular units were within the standard deviations. The best refinement was obtained by fixing the occupation factor of the oxygen atom of the radical NITMe, substituted by a hydrogen atom in the reduced form IMHMe, to a value of 0.5. The hydrogen atoms were introduced in fixed and idealized positions with thermal factors about 20% greater than that of the respective carbon atom. The refinement with 1780 reflections $F_o \geq 4\sigma(F_o)$ converged to $R = 0.052$ and $R_w = 0.058$. The final atomic positional parameters are listed in Table II.

Magnetic Susceptibility Measurements. Magnetic susceptibilities were measured for both compounds in the temperature range 300–5 K by using an SHE superconducting SQUID susceptometer at a field strength of 0.01 T.

Electron Paramagnetic Resonance Measurements. Variable-temperature EPR spectra of polycrystalline powder of both compounds and of

a single crystal of compound II were recorded with a Varian E9 spectrometer operating at X-band and equipped with an Oxford Instruments ESR9 continuous-flow cryostat.

Results

Synthesis of the Complexes. When $\text{Mn}(\text{pfpr})_2$ is reacted in chloroform solution with NITMe, two different solids can be isolated depending on the concentration of reagents, reaction temperature, and presence of impurities in the solvent. When the solids are allowed to precipitate slowly, i.e. from dilute solution and relatively high temperature, practically one crystalline compound of formula $[\text{Mn}(\text{pfpr})_2]_2(\text{NITMe})(\text{IMHMe})$ is obtained. The formation of the compound is made easier if the solvent contains some acidic impurity.¹⁷ At relatively high concentrations and low temperature, in carefully purified chloroform, a polycrystalline compound of formula $\text{Mn}(\text{pfpr})_2(\text{NITMe})$ is obtained. When the experimental conditions are intermediate between these limits both compounds are obtained.

The correct formulation of I and II cannot be made on the basis of the elemental analysis but rather by using additional evidence coming from several physicochemical techniques, as shown below.

The presence of IMHMe in II was unambiguously characterized by chromatographic techniques. The compound was dissolved in CH_2Cl_2 and the resulting solution eluted on an alumina thin layer, giving two spots, one being colored and having the same R_f and the same solution EPR spectrum as NITMe. The colorless spot, which has a lower R_f , was oxidized with sodium metaperiodate¹⁶ and eluted with CH_2Cl_2 to give an orange spot whose solution EPR spectrum is identical with that of an authentic sample of IMMe. Therefore, the colorless spot was assigned to the reduced form of IMMe, IMHMe. It is worth noting that, in the same conditions, compound I gives only one spot corresponding to NITMe.

Further evidence for the 1:1 ratio of NITMe to IMHMe in II is obtained from comparison of the UV-visible spectra of I and II. The radical NITMe is characterized by two medium-intensity absorptions in the visible region, with maxima near $18\,000\text{ cm}^{-1}$, which can be assigned to a $n \rightarrow \pi^*$ transition.^{16,17} The molar absorption coefficients are ca. $1800\text{ cm}^{-1}\text{ mol}^{-1}$. Since both I and II are completely dissociated in solution and IMHMe has no absorption in the $18\,000\text{-cm}^{-1}$ region, the UV-vis spectrum can be used to monitor the relative quantities of NITMe in I and II. The spectra show that the manganese-radical ratio is 1.00 ± 0.05 for I and 2.00 ± 0.05 for II. Analogous results can be obtained by the analysis of the EPR spectra in aqueous solution, which show the presence of the NITMe radical. No evidence of the presence of the IMMe radical is found.

As mentioned above, the reduced form of NITMe can exist in two tautomeric forms.^{16,17} Since the oxygen atom is here involved in bonding two manganese ions, the amidino-oxide form is the more probable one, as confirmed by the IR spectra of II, which show a broad absorption at ca. 3350 cm^{-1} in agreement with a N-H stretching.

The conversion of NITMe into IMHMe has been already observed in the presence of manganese(II) salts in heptane at high temperature,¹⁸ and also in that case the amidino-oxide form was found to bind to the metal ion. The reduction from NITR to IMHR has been shown to be promoted by acidic species.^{17,22,23} It is very likely that the formation of IMHMe, in the present case, is favored both by the temperature and acidic impurities, which are usual in reagent grade chloroform. The experimental conditions for obtaining compounds I and II are indeed in agreement with these considerations.

Crystal Structure of II. The asymmetric unit of II is shown in Figure 1. The manganese ions are coordinated by four oxygen atoms of four carboxylates, each pair of carboxylates bridging in a μ -1,3 fashion two manganese ions. The manganese carboxylates

(21) Sheldrick, G. SHELX 76 System of Computing Program. University of Cambridge, Cambridge, England, 1976. Atomic scattering factors: Cromer, D. T.; Liberman, D. J. *J. Chem. Phys.* **1970**, *53*, 1891.

(22) Forrester, A. R.; Hay, J. M.; Thomson, R. H. In *Organic and Inorganic Chemistry of Stable Free Radicals*; Academic Press: London, 1968; p 180.

(23) Rozantsev, E. G. *Free Nitroxyl Radicals*; Plenum Press: New York, 1970.

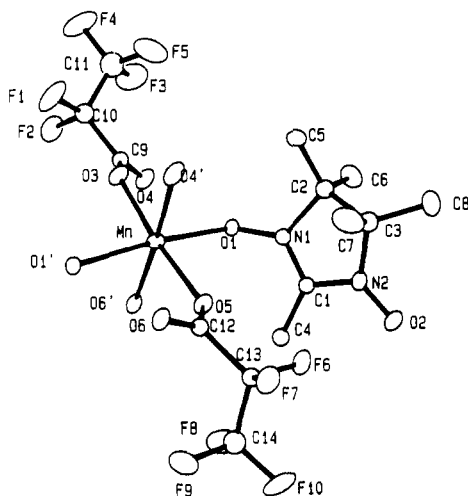


Figure 1. ORTEP view of the asymmetric unit of $[\text{Mn}(\text{pfpr})_2]_2(\text{NITMe})(\text{IMHMe})$ (II). The occupation factor of O2 has been fixed to 0.5.

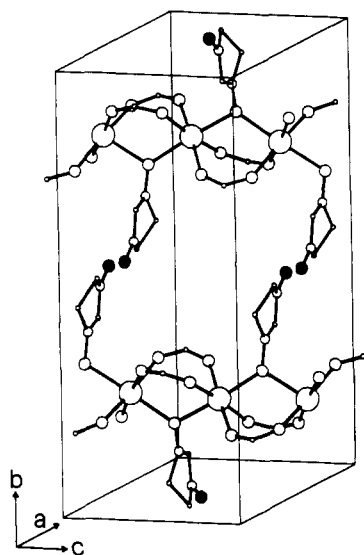


Figure 2. View of the unit cell of $[\text{Mn}(\text{pfpr})_2]_2(\text{NITMe})(\text{IMHMe})$, showing the chain structure and the contacts between chains. For the sake of clarity the CF_3 and CH_3 groups were omitted. The filled circles represent the disordered sites half-occupied by oxygen and hydrogen atoms.

form a one-dimensional array parallel to c , as shown in Figure 2. The octahedral coordination environment of the manganese ions is completed by two equivalent oxygen atoms, related by the glide plane, belonging to NO groups that bridge in a μ -1,1 fashion two manganese ions. These belong either to NITMe or IMHMe, but the difference between them, the former possessing two NO groups and the latter one NO group and one NH group, shows up only as disorder on the side of the molecule that is far from the manganese ion, the thermal parameters of the other atoms of the disordered molecule being about normal. The electron density observed in the far end of the molecule (referred to the manganese ion) is roughly intermediate between that of an oxygen and of a hydrogen atom, and satisfactory refinement of the structure could be performed by assuming random occupation of oxygen and hydrogen atoms, with equal statistical weight.

These disordered atoms, labeled as O2, have a short contact of 1.8 Å with the analogous atoms of a neighboring chain, related by an inversion center, suggesting a hydrogen bond. The N2–O2 distance is 1.23 (1) Å, and the distance of O2 from the nitrogen atom of the molecule in the neighboring chain is 2.93 (1) Å, which again agrees with a hydrogen bond (Table III). In the following we will analyze the bond distances involving the molecules with five-membered rings as intermediate between a NITMe and an IMHMe.

Table III. Selected Bond Distances (Å) and Angles (deg) in $[\text{Mn}(\text{pfpr})_2]_2(\text{NITMe})(\text{IMHMe})^a$

Distances			
Mn–O1	2.331 (4)	Mn–O1'	2.290 (4)
Mn–O3	2.114 (5)	Mn–O4'	2.146 (5)
Mn–O5	2.163 (5)	Mn–O6'	2.152 (5)
O1–N1	1.350 (4)	O2–N2	1.229 (12)
O3–C9	1.228 (5)	O4–C9	1.240 (6)
O5–C12	1.238 (5)	O6–C1	1.241 (4)
N1–C1	1.306 (1)	N1–C2	1.517 (1)
N2–C1	1.355 (6)	N2–C3	1.490 (6)
Angles			
O5–Mn–O6'	90.9 (2)	O4'–Mn–O6'	176.1 (2)
O4'–Mn–O5	88.9 (2)	O3–Mn–O6'	96.2 (2)
O3–Mn–O5	172.4 (2)	O3–Mn–O4'	84.0 (2)
O1'–Mn–O6'	87.2 (2)	O1'–Mn–O5	87.7 (2)
O1'–Mn–O4'	89.0 (2)	O1'–Mn–O3	95.1 (2)
O1–Mn–O6'	86.3 (2)	O1–Mn–O5	91.1 (2)
O1–Mn–O4'	97.5 (2)	O1–Mn–O3	86.8 (2)
O1–Mn–O1'	173.4 (2)	Mn–O1–Mn	116.7 (2)
Mn'–O1–N1	124.2 (3)	Mn–O1–N1	117.0 (3)

^a Standard deviations in the last significant digit are in parentheses.

The Mn–O distances involving the carboxylates are shorter than those involving the disordered molecules. The latter are longer than those observed in $\text{Mn}(\text{pfpr})_2(\text{NITet})_2(\text{H}_2\text{O})_3$,¹⁰ where the nitroxide is bound in a terminal position (2.331 (4) and 2.290 (4) vs 2.164 (6) Å), and also longer than observed in $[\text{Mn}(\text{hfac})_2(\text{IMHPh})_2]_2(\text{NITPh})$ and $\text{Mn}(\text{hfac})_2(\text{IMHPh})(\text{IMPh})$,¹⁸ where the analogous reduced form of the NITPh radical bridges two manganese ions. In that case in fact the Mn–O distance is 2.15 Å.

The N1–O1 distance of 1.350 (4) Å is intermediate between that observed in complexes with coordinated NITR radicals (1.26–1.29 Å)^{3,5,7,10,24} and in complexes with coordinated IMHPh (1.37–1.39 Å).¹⁸ On the other hand, the distance between N2 and O2 is 1.229 (12) Å, significantly shorter than that observed for a radical.^{3,5,7,10,24} The N2–C1 and N1–C1 distances are rather similar to those observed for coordinated radicals^{3,5,7,10,24} and IMHPh molecules.¹⁸

The presence of the O–H–N hydrogen bonds between NITMe and IMHMe allows each chain to be connected to two neighboring chains in such a way that they define a puckered plane orthogonal to a .

Magnetic Properties. For both I and II the χT vs T plots increase on decreasing temperature, as shown in Figure 3. The susceptibility is referred to one manganese atom in both cases. The room-temperature values are 4.83 emu K mol⁻¹ ($\mu_{\text{eff}} = 6.2 \mu_{\text{B}}$) for I and 3.84 emu K mol⁻¹ ($\mu_{\text{eff}} = 5.5 \mu_{\text{B}}$) for II. The increase is much more marked for I than for II: while for the latter the highest value does not exceed 7 emu K mol⁻¹, for I values as high as 18 emu K mol⁻¹ are reached. Both curves reach a maximum and then decrease at low temperature, but for I even the χ vs T plot passes through a maximum at 7 K.

EPR Spectra. Polycrystalline powder EPR spectra of both I and II at room temperature show one isotropic feature at $g = 2$, with line widths 100 and 125 G, respectively. Single crystal spectra of II were recorded at room temperature by rotating around the c axis, the axis orthogonal to the (110) face, and a third axis orthogonal to the other two. The spectra have anisotropic line width, with a maximum parallel to the chain direction c , a minimum at the magic angle, and an additional maximum orthogonal to c , as shown in Figure 4. With rotation around c it is apparent that the line goes to a minimum parallel to a and to a maximum parallel to b . A weak signal is also observed at half-field. The line is Lorentzian at all angular settings.

On decreasing temperature the line width decreases to a minimum close to 100 K. Below this value the line width increases. At 4 K the lines are so broad that no single-crystal spectra could

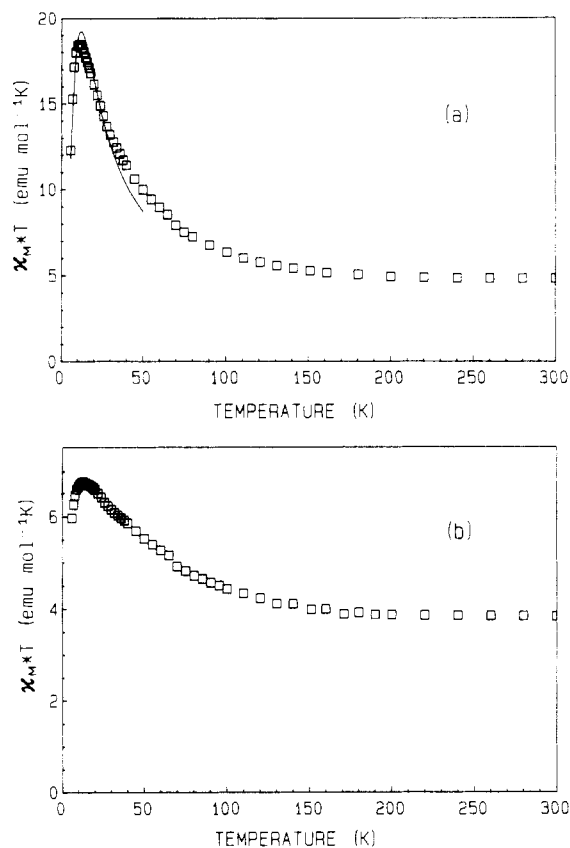


Figure 3. Variation of the magnetic susceptibility in the form χT with the temperature for $\text{Mn}(\text{pfpr})_2(\text{NITMe})$ (a) and $[\text{Mn}(\text{pfpr})_2]_2(\text{NITMe})(\text{IMHMe})$ (b). The solid line in (a) represents the calculated value (see text).

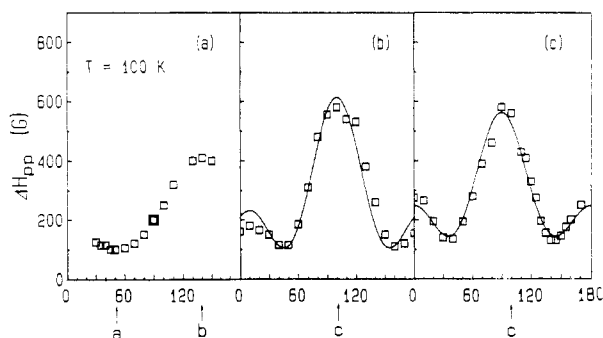


Figure 4. Angular dependence of the peak-to-peak line width of the EPR spectra at room temperature of a single crystal of $[\text{Mn}(\text{pfpr})_2]_2(\text{NITMe})(\text{IMHMe})$ rotated along three orthogonal axes (see text). The solid lines are calculated by the equation $\Delta H_{pp} = a + b(3 \cos^2 \theta - 1)^2$, where θ is the angle of the magnetic field with the chain direction c .

be recorded. No g shift was observed at low temperature.

Discussion

The crystal structure of II is an important example of how one-dimensional polymers can spontaneously organize into a two-dimensional structure through a network of hydrogen bonds. The N-O and N-H ends of NITMe and IMHMe, respectively, act as conjugate bold-lock pairs that keep the neighboring chains tightly bound to each other. The disorder observed in the structure suggests that there is a random distribution of NITMe and IMHMe molecules, but whenever one is present, the complementary molecule must be present in the neighboring chain. Therefore, the disorder has still some ordered character in itself. In other terms, the presence of two different molecules that alternate in the lattice allows the chains to exchange information between themselves. The main consequence is that this kind of structure requires equal numbers of NITMe and IMHMe molecules.

In principle the disorder of the NITMe and IMHMe molecules can be of two kinds: (i) the NITMe radicals are randomly distributed along the chains; (ii) the NITMe radicals are in one chain, with the IMHMe molecules in the neighboring chains. In this way the disorder should be between planes, i.e. within a plane an ordered array of $\text{Mn}(\text{pfpr})_2(\text{NITMe})$ and $\text{Mn}(\text{pfpr})_2(\text{IMHMe})$ is present, but on neighboring planes the translational symmetry is not conserved. Alternative i seems to be more probable on the basis of entropy considerations and of the similarity of the Lewis basicity of the two ligands, and also the magnetic properties concur to the same indication.

When the manganese ions are bridged by NITMe, the coupling between the metal ion and the radical is expected to be antiferromagnetic and of the order of 10^2 cm^{-1} ,^{2,24} where the spin Hamiltonian is defined as $H = JS_1S_2$, while when the manganese ions are bridged by IMHMe, the metal-metal antiferromagnetic coupling must be of the order of 10^0 cm^{-1} .¹⁸ As a consequence, the magnetic properties corresponding to alternative ii should be given by the sum of the contribution of ferrimagnetic chains are connected by hydrogen bonds, only weak coupling between the two would be expected. In fact this was found to be the case in $[\text{Mn}(\text{hfac})_2(\text{IMHPh})]_2(\text{NITPh})$ and in $\text{Mn}(\text{hfac})_2(\text{IMHPh})(\text{IMPh})$.¹⁸ Therefore, the magnetic susceptibility of II should be fitted by a model which averages the contribution of the $\text{Mn}(\text{pfpr})_2(\text{NITMe})$ chains as that of coupled classic-quantum spin ferrimagnetic chains,²⁵ and that of $\text{Mn}(\text{pfpr})_2(\text{IMHMe})$ as that of antiferromagnetic $S = 5/2$ chains.²⁶ Attempts were made to fit the experimental data with this model, but they were unsuccessful.

If we assume that in II the NITMe and IMHMe molecules are randomly distributed along the chains, these can be considered as impurity-doped one-dimensional magnetic materials. This problem has already been studied in one-dimensional antiferromagnets, such as $[\text{N}(\text{Me})_4]\text{MnCl}_3$, TMMC, which has been doped with either paramagnetic or diamagnetic metal ion with the purpose to determine the relevance of doping to spin diffusion along the chains.²⁷⁻²⁹ The effect of disorder has also been taken into consideration for one-dimensional organic radical chains.³⁰

The statistical distribution of NITMe and IMHMe molecules along the chains can be calculated by using the formula³¹

$$p_m = N(1-x)^m x^2 \quad (1)$$

where p_m is the probability of finding an array of m neighboring molecules of the same type, N is the total number of sites, and x is the ratio of molecules of one kind to the total number of molecules. In the present case $x = 0.5$. An accurate calculation of the magnetic susceptibility seems to be impossible in this case, but a limit value for low temperature can be evaluated through a simplified model. We assume that the exchange through the IMHMe bridges is negligibly small. We know that this is not the case, because the comparison with other similar compounds suggests that it can be of the order of 10^0 cm^{-1} ,¹⁸ but using this simplification, we overestimate the χT value at low temperature. The exchange between the manganese ions bridged by NITMe radicals on the other hand will be strongly antiferromagnetic, with J of the order of 10^2 cm^{-1} , as observed in other analogous complexes.^{2,4,7,10,24} Therefore, the total spin state of the segments in which manganese ions are bridged by radicals can be calculated by assuming that all the manganese spins are up and the radical spins down. The contribution to χT of an array of m NITMe molecules can be calculated by considering that it comprises m

(25) Seiden, J. J. *Phys. Lett.* **1983**, *44*, L947.

(26) Fisher, M. E. *Am. J. Phys.* **1964**, *32*, 3243.

(27) Lauer, C.; Benner, H. *Phys. Rev. B* **1981**, *24*, 329.

(28) Clement, S.; Renard, J.-P.; Ablart, G. *J. Magn. Reson.* **1984**, *60*, 46.

(29) Tazuke, Y. *J. Phys. Soc. Jpn.* **1977**, *42*, 1617.

(30) Soos, Z. G.; Bondeson, S. R. In *Extended Linear Chain Compounds*; Miller, J. S., Ed.; Plenum Press: New York, 1983; Vol. 3, p 233. Bulaevskii, L. N.; Zvarykina, A. V.; Rarimov, Y. S.; Lyubovskii, R. B.; Shchegolev, I. F. *Sov. Phys.—JEPT (Engl. Transl.)* **1972**, *35*, 384.

(31) Amoretti, G.; Buluggiu, E.; Vera, A.; Colestani, G.; Maticotto, F. C. *Z. Phys. B* **1988**, *72*, 17.

+ 1 manganese ions. By definition the terminal manganese ions at the two ends of the array are connected to other manganese ions through IMHMe molecules that break the coupling. Therefore, the contribution to χT of these clusters of m NITMe radicals and $m + 1$ manganese ions is that of a system with total spin $S = (m + 1)^2/2 - m/2$. On the whole, there will be $N/2$ manganese ions in this condition, while the remaining ones, sandwiched by IMHMe molecules, contribute $4.375 \text{ emu K mol}^{-1}$ each to χT . With this model the limit of χT at 0 K is calculated to be $8.18 \text{ emu K mol}^{-1}$. The highest experimental value of χT of II, smaller than this limit, indicates that the model is useful to give an idea of the magnetic interactions present in II.

The single-crystal EPR spectra have the characteristic angular dependence of the line width of one-dimensional magnetic materials,^{6,32,33} with a maximum along the chain and a minimum at the magic angle. This behavior is determined by spin-diffusion effects along the chain, and it shows that the chains are essentially not broken; i.e., the spin can move freely also through the IMHMe bridges. The maximum line width observed along the chain direction can be justified by a dipolar broadening mechanism determined by the manganese-manganese interaction. Along this line it can also be justified the fact that the second highest maximum is observed parallel to b , which corresponds to the manganese-radical direction.

The crystal structure of I is not known, but the stoichiometry and the magnetic data suggest that ferrimagnetic chains are formed with bridging NITMe groups, as observed in II. Indeed the χT data down to ca. 30 K can be fit with the formulas appropriate to one-dimensional $S = 5/2$ to $S = 1/2$ ferrimagnets,²⁵ with $g = 2$ and $J = 110 \text{ cm}^{-1}$. The calculated value of the coupling constant is smaller than that observed in other compounds in which manganese(II) ions are coupled to nitronyl nitroxides.^{4,7,24} However, it must be noticed that in all the previously reported compounds the nitronyl nitroxides bind to one manganese ion through one of their oxygen atoms, while in this case we suggest an oxygen atom bridging two manganese ions, and this may reduce the extent of the antiferromagnetic coupling. In the case of nickel(II) compounds with nitronyl nitroxides we found that J drops from ca. 400 cm^{-1} when the radicals bind in a $\mu-1,3$ way⁵ to ca. 300 cm^{-1} when they bind in a $\mu-1,1$ fashion.³⁴ In simple dinuclear manganese(II) complexes bridged by two $\mu-1,1$ -nitronyl nitroxides, J was found to be ca. 130 cm^{-1} .³⁵

The maximum that we observe in the χ vs T plot is a clear indication of a substantial interchain coupling of antiferromagnetic character. We suggest that this may be due to short contacts between the NO groups of the NITMe molecules that are not bound to the manganese ions. In other words we suggest for I a structure which is similar to that of II, with the obvious difference that the absence of interchain hydrogen bonds allows only for relatively weak NO-ON contacts, as observed in other compounds in which the nitronyl nitroxides have noncoordinated NO groups.^{34,36,37}

The scheme of the magnetic interactions according to the suggested structure is shown in Figure 5a. The material is two-dimensional, with large coupling within the chains and weak coupling between the chains. A simple model can be developed by using classic spins along the chain: at a given temperature the effective total spin per manganese-radical pair can be calculated as

$$S_{\text{eff}}(T) = -1/2 + 1/2\sqrt{1 + 8\chi_{\text{ch}}T} \quad (2)$$

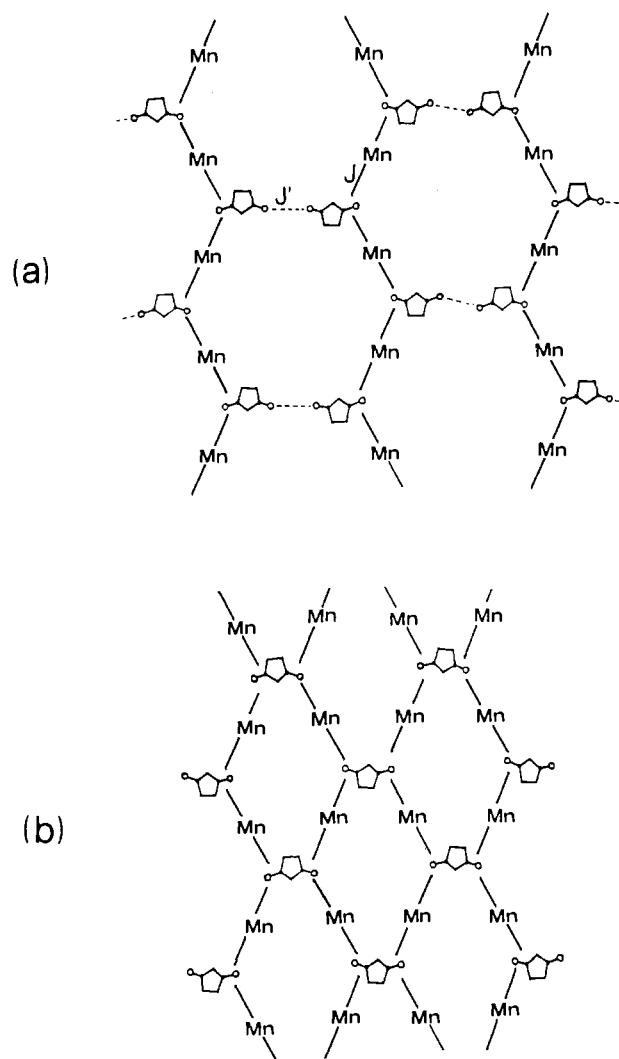


Figure 5. Scheme of the supposed magnetic interactions present in $\text{Mn}(\text{pfpr})_2(\text{NITMe})$ (a) and in $[\text{Mn}(\text{pfbz})_2]_2(\text{NITR})$ (b). Scheme (a) has been used to fit the magnetic data of I below 50 K.

where χ_{ch} is the susceptibility calculated with the classic-quantum model for ferrimagnetic chains.²⁵ The susceptibility for the material is then calculated with the expression for antiferromagnetic chains²⁶ with total spin $S_{\text{eff}}(T)$. In other terms we calculate the susceptibility of the two-dimensional magnet as that of a chain of chains. The best fit values are $J = 104$ (4) cm^{-1} and $J' = 0.052$ (2) cm^{-1} , and the calculated susceptibility is reported in Figure 3. The J value is similar to that calculated for the high-temperature data, while the J' value agrees with a weak coupling between chains. This simple model fits also the observed maximum in the susceptibility observed at 7 K, while a molecular field correction to the one-dimensional susceptibility is unable to reproduce it.

Conclusions

The use of manganese carboxylates instead of manganese hexafluoroacetylacetonates allowed us to increase the dimensionality of the magnetic materials formed with nitronyl nitroxides. In fact the carboxylates provide a one-dimensional backbone, leaving the possibility for nitronyl nitroxides to connect different chains. Up to now we have been able to obtain suitable crystals for X-ray analysis only in the case of II, where the radical has been partially reduced. It is certainly interesting from a general chemical point of view to see how in this compound the one-dimensional backbone is connected by pairs of molecules through hydrogen bonds, which force two neighboring chains to have complementary structures. The comparison with DNA appears obvious, even if the complexity of this system is certainly much lower.

- (32) Richards, P. M. In *Local Properties at Phase Transitions*; Editrice Compositori: Bologna, Italy, 1975.
- (33) Gatteschi, D.; Sessoli, R. *Magn. Reson. Rev.* **1990**, *15*, 1.
- (34) Caneschi, A.; Gatteschi, D.; Laugier, J.; Rey, P.; Sessoli, R. *Inorg. Chem.* **1988**, *27*, 1553.
- (35) Benelli, C.; Caneschi, A.; Gatteschi, D.; Melandri, M. C. *Inorg. Chim. Acta* **1990**, *172*, 137.
- (36) Laugier, J.; Rey, P.; Gatteschi, D.; Zanchini, C. *J. Am. Chem. Soc.* **1986**, *108*, 6931.
- (37) Caneschi, A.; Ferraro, F.; Gatteschi, D.; Rey, P.; Sessoli, R. *Inorg. Chem.* **1990**, *29*, 1756.

The structure of I cannot be too dissimilar from that of II, in the sense that the interchain interactions are developed presumably through NO-NO contact but keeping the two-dimensional structure. This is unfortunate, because the interaction is antiferromagnetic, and ferromagnetic three-dimensional order cannot be achieved in this way.

However, this does not mean that the use of carboxylates cannot lead to molecular based ferromagnets. Indeed we have observed relatively high transition temperatures⁹ to three-dimensional magnetic order in $[\text{Mn}(\text{pfbz})_2]_2(\text{NITR})$. The fact that we could not obtain suitable single crystals made the analysis of the magnetic phase transition not unambiguous, but there is an indication for either a weak ferro or ferrimagnetic transition. We can now suggest that $[\text{Mn}(\text{pfbz})_2]_2(\text{NITR})$ has a two-dimensional structure which can be obtained from that of II, by substituting each NITMe-IMHMe conjugate pair with one NITR radical.

In this way the scheme of magnetic structure given in Figure 5b would ensure a two-dimensional ferrimagnetic structure. The relatively high transition temperature observed in this case, in the range 20-25 K,⁹ compared to that of the one-dimensional materials,^{5,7} in the range 4-8 K, would be justified by the increased magnetic dimensionality.

Acknowledgment. The financial support of the CNR, of the Progetto Finalizzato "Materiali Speciali per Tecnologie Avanzate", and of MURST is gratefully acknowledged.

Supplementary Material Available: Tables SI-SV, listing crystallographic and experimental parameters, calculated positions of hydrogen atoms, anisotropic thermal factors, and bond distances and angles, and Figure S1, showing a schematic view of the puckered planes formed by hydrogen bonds (9 pages); Table SVI, listing observed and calculated structure factors (9 pages). Ordering information is given on any current masthead page.

Contribution from the Department of Physics, The Pennsylvania State University, University Park, Pennsylvania 16802, and the Departments of Chemistry, University of Southern California, Los Angeles, California 90089-0744, and University of Notre Dame, Notre Dame, Indiana 46556

Mossbauer and Magnetic Susceptibility Investigation of a Ferromagnetically Coupled Iron(III) Porphyrin-Dicopper(II) System with Imidazolate Bridging Ligands

Govind P. Gupta,^{†,‡} George Lang,^{*,†} Carol A. Koch,[§] Bing Wang,[§] W. Robert Scheidt,^{||} and Christopher A. Reed^{*,§}

Received March 22, 1990

Susceptibility and Mossbauer techniques were employed to analyze the magnetic properties of the trinuclear complex $[\text{Fe}^{\text{III}}(\text{TPP})(\text{CuIM})_2]\text{B}_{11}\text{CH}_{12}\cdot 5\text{THF}$ (TPP = tetraphenylporphyrinate; CuIM = copper(II) complex of the Schiff base formed by sequential condensation of 5-chloro-2-hydroxybenzophenone, 1,2-diaminobenzene, and imidazole-4-carbaldehyde). The Fe(II) analogue (magnetic Fe(III) ions replaced by diamagnetic Fe(II) ions) and its Ni analogue (magnetic Cu ions replaced by diamagnetic Ni ions) were studied. Susceptibility measurements on the Fe(II) analogue in 10-kG magnetic field showed that the effective magnetic moment above 20 K remains $2.60 \mu_{\text{B}}$, which would correspond to two Cu ions with $S = 1/2$ and $g_{\text{Cu}} = 2.12$. The magnetic moment below 20 K decreases significantly and was fitted with pairwise antiferromagnetic coupling with $J_{\text{CuCu}} = -1.52 \text{ cm}^{-1}$. The diamagnetic character of Fe(II) was confirmed by Mossbauer spectroscopy. In the Ni analogue, $[\text{Fe}^{\text{III}}(\text{TPP})(\text{NiIM})_2]\text{B}_{11}\text{CH}_{12}\cdot 5\text{THF}$, the effective magnetic moment at 300 K is $2.2 \mu_{\text{B}}$ and remains around $2 \mu_{\text{B}}$ down to 2 K. The susceptibility and Mossbauer data were fitted with a $S = 1/2$ model with axial field $\Delta/\lambda = 5$, rhombicity $V/\Delta = 0.4$, and one-electron spin-orbit coupling constant $\lambda = 400 \text{ cm}^{-1}$, corresponding to $g_{\text{Fe}} = 1.63, 2.14, \text{ and } 2.90$. The analysis of its Mossbauer spectra also provides $\delta = 0.24 \text{ mm/s}$, $\Delta E = -2.26 \text{ mm/s}$, $\eta = 0.1$ (where the principal EFG axis is along the x magnetic axis), and $P_{\text{K}}/(g_{\text{N}} \mu_{\text{N}}) = 17.0 \text{ T/unit spin}$. All parameters are consistent with the $S = 1/2$ character of this system. The effective magnetic moment of $3.4 \mu_{\text{B}}$ found for $[\text{Fe}^{\text{III}}(\text{TPP})(\text{CuIM})_2]\text{B}_{11}\text{CH}_{12}\cdot 5\text{THF}$ at 300 K corresponds to a susceptibility that is the sum of those of its two analogues. However, as the temperature is decreased, the effective moment rises to a maximum at 8 K, indicating ferromagnetic Fe-Cu coupling. This can be understood in terms of a σ/π orthogonality of the magnetic orbitals. The analysis of the susceptibility data measured in the temperature range 2-300 K reveals ferromagnetic exchange of $J_{\text{FeCu}} = 22.2 \text{ cm}^{-1}$, making a Cu-Fe-Cu type molecular spin, and an antiferromagnetic chainlike coupling of $J_{\text{CuCu}} = -1.87 \text{ cm}^{-1}$ between such molecular spins. High-field Mossbauer data are consistent with this interpretation. The zero-field Mossbauer parameters ($\delta = 0.23$ and $\Delta E = -2.07 \text{ mm}\cdot\text{s}^{-1}$) are very similar to those of the Ni analogue and are unaffected by spin coupling to copper.

Introduction

In a recent communication, we reported the first example of ferromagnetic coupling via an imidazolate bridging ligand.¹ The significance of this result lies in its support for the concept of orthogonal magnetic orbitals,² which is becoming an increasingly powerful rationale for intramolecular ferromagnetic interactions. The system involves the bis coordination of a copper(II) imidazolate chelate (CuIM) to a low-spin iron(III) tetraphenylporphyrin cation to give the trimetallic unit shown in Figure 1. The ferromagnetic interaction arises from a σ/π symmetry mismatch of the $d_{x^2-y^2}$ orbital on copper and the d_{yz} orbital on iron. The magnitude of the coupling, $J_{\text{FeCu}} = +22 \text{ cm}^{-1}$, is surprisingly large considering the $>6\text{-\AA}$ separation of the metal atoms.

In addition to the intramolecular ferromagnetic interaction, there is an antiferromagnetic interaction between cations in the

lattice, which adds a complexity to the system. However, by the complementary application of magnetic susceptibility measurements and Mossbauer spectroscopy, an overall magnetic coupling model can be developed. The details of this analysis are the main subject of this report. A number of features of the electronic structure of the system emerge from the analysis, and a linear-chain intermolecular interaction is required to rationalize the antiferromagnetic coupling component.

The broader significance of this work lies in its relation to models for the heme a_3/Cu_B site of cytochrome oxidase. MCD measurements on the cyanide form of this enzyme have been interpreted in terms of ferromagnetic coupling between iron(III) and copper(II),³ and this conclusion is consistent with Mossbauer results.⁴ A σ/π orthogonality of magnetic orbitals with respect

[†] The Pennsylvania State University.

[‡] On leave from Lucknow University, Lucknow, India.

[§] University of Southern California.

^{||} University of Notre Dame.

(1) Koch, C. A.; Reed, C. A.; Brewer, G.; Rath, N. P.; Scheidt, W. R.; Gupta, G. P.; Lang, G. J. *Am. Chem. Soc.* **1989**, *111*, 7645.

(2) Kahn, O.; Galy, J.; Journaux, Y.; Jaud, J.; Morgenstern-Badarau, I. J. *Am. Chem. Soc.* **1982**, *104*, 2165.

(3) Thomson, A. J.; Johnson, M. K.; Greenwood, C.; Gooding, P. E. *Biochem. J.* **1980**, *193*, 687.